Insect Biochemistry and Molecular Biology 104 (2019) 73–81

Contents lists available at ScienceDirect

Insect Biochemistry and Molecular Biology

journal homepage: www.elsevier.com/locate/ibmb

Functional validation of target-site resistance mutations against sodium channel blocker insecticides (SCBIs) via molecular modeling and genome engineering in *Drosophila*

George-Rafael Samantsidis[a,b,1], Andrias O. O'Reilly[c,1], Vassilis Douris[a,*], John Vontas[a,d,**]

[a] Institute of Molecular Biology & Biotechnology, Foundation for Research & Technology Hellas, 100 N. Plastira Street, GR-700 13, Heraklion Crete, Greece
[b] Laboratory of Molecular Entomology, Department of Biology, University of Crete, GR-700 13, Heraklion Crete, Greece
[c] School of Natural Sciences and Psychology, Liverpool John Moores University, Liverpool, UK
[d] Laboratory of Pesticide Science, Department of Crop Science, Agricultural University of Athens, 75 Iera Odos Street, GR-11855, Athens, Greece

ARTICLE INFO

Keywords:
Sodium channels
Insecticide resistance
CRISPR/Cas9
Molecular modeling
Indoxacarb
Metaflumizone

ABSTRACT

Sodium channel blocker insecticides (SCBIs) like indoxacarb and metaflumizone offer an alternative insecticide resistance management (IRM) strategy against several pests that are resistant to other compounds. However, resistance to SCBIs has been reported in several pests, in most cases implicating metabolic resistance mechanisms, although in certain indoxacarb resistant populations of *Plutella xylostella* and *Tuta absoluta,* two mutations in the domain IV S6 segment of the voltage-gated sodium channel, F1845Y and V1848I have been identified, and have been postulated through *in vitro* electrophysiological studies to contribute to target-site resistance.

In order to functionally validate *in vivo* each mutation in the absence of confounding resistance mechanisms, we have employed a CRISPR/Cas9 strategy to generate strains of *Drosophila melanogaster* bearing homozygous F1845Y or V1848I mutations in the *para* (voltage-gated sodium channel) gene. We performed toxicity bioassays of these strains compared to wild-type controls of the same genetic background. Our results indicate both mutations confer moderate resistance to indoxacarb (RR: 6–10.2), and V1848I to metaflumizone (RR: 8.4). However, F1845Y confers very strong resistance to metaflumizone (RR: > 3400). Our molecular modeling studies suggest a steric hindrance mechanism may account for the resistance of both V1848I and F1845Y mutations, whereby introducing larger side chains may inhibit metaflumizone binding.

1. Introduction

Voltage-gated sodium channels (VGSCs) conduct sodium ions across the plasma membrane of neurons to generate and propagate electrical signals, which facilitate an animal's movement and response to various environmental stimuli (see review by Carnevale and Klein, 2017). VGSC α-subunits are comprised of four homologous domains (I-IV), each having six membrane spanning helical segments (S1−S6) (Catterall, 2017). Recent VGSC structures determined by cryo-electron microscopy reveal how pore gating is coupled with movement of the voltage sensors that detect transmembrane potential changes (Shen et al., 2017, 2018; Yan et al., 2017). A continuous ion-conducting pathway through the pore is found in the open-state electric eel VGSC structure (Yan et al., 2017) as the pore-lining S6 helices are dilated at the cytoplasmic entrance.

VGSCs are the primary targets of many inhibitory chemicals such as local anesthetics (analgesics, antirrhythmic drugs) in vertebrates as well as chemical insecticides in insects that suppress neurons' excitability and their high-frequency discharges (Gawali et al., 2015). Indoxacarb (a pyrazoline type insecticide) and metaflumizone (Fig. 1) belong to the family of Sodium Channel Blocker Insecticides (SCBIs; von Stein et al., 2013) that bind to the open channel pore when the membrane is still depolarized and cause a shift in the voltage dependence of slow inactivation to more negative potentials. Thus, VGSCs are stabilized in the inactivated state leading to termination of the intracellular sodium influx (Silver and Soderlund, 2007; Silver et al., 2010, 2017; Jiang et al.,

* Corresponding author. Institute of Molecular Biology & Biotechnology, Foundation for Research & Technology Hellas, 100 N. Plastira Street, GR-700 13, Heraklion Crete, Greece.
** Corresponding author. Institute of Molecular Biology & Biotechnology, Foundation for Research & Technology Hellas, 100 N. Plastira Street, GR-700 13, Heraklion Crete, Greece.
E-mail addresses: vdouris@imbb.forth.gr (V. Douris), vontas@imbb.forth.gr (J. Vontas).
[1] These authors contributed equally to this work.

https://doi.org/10.1016/j.ibmb.2018.12.008
Received 19 September 2018; Received in revised form 14 December 2018; Accepted 14 December 2018
Available online 17 December 2018
0965-1748/

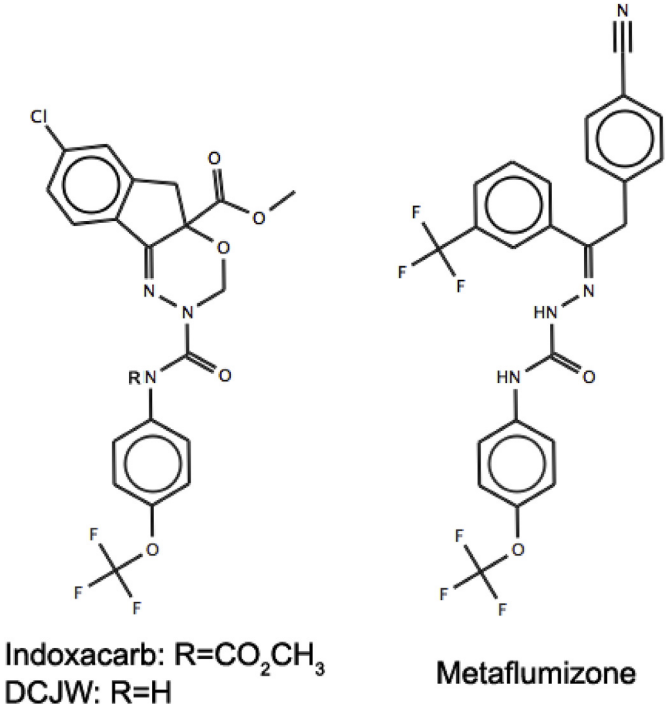

Fig. 1. Chemical structures of sodium channel blocker insecticides.

2015; Zhang et al., 2016).

Indoxacarb is an insecticidal oxadiazine (Fig. 1) characterized as a pro-insecticide since it has to be converted to the active metabolite N-decarbomethoxylated JW062 (DCJW), a secondary product generated by the hydrolyzing activity of insect esterases or amidases, which underlies its action selectivity against insects (Zhang et al., 2016). Indoxacarb is used against moths, beetles, leafhoppers, weevils, flies and other pests (Silver et al., 2010). Spraying treatment of *Drosophila* with DCJW is also effective and eventually causes mortality (Zhang et al., 2013). Metaflumizone belongs to the category of semicarbazones, which are ring-opened dihydropyrazoles (von Stein et al., 2013) (Fig. 1). Metaflumizone exhibits low toxicity to mammals and selectivity towards insects (Hempel et al., 2007) and, unlike indoxacarb, it does not require metabolism to produce the active compound.

Resistance against SCBIs have been reported in insects such as the housefly *Musca domestica* (Shono et al., 2004), the lepidopteran pests *Choristoneura rosaceana* (Ahmad et al., 2002), *Plutella xylostella* (Khakame et al., 2013; Wang et al., 2016; Zhang et al., 2017), *Spodoptera exigua* (Tian et al., 2014), *Helicoverpa armigera* (Bird et al., 2017) and *Tuta absoluta* (Roditakis et al., 2017) and the cockroach *Blatella germanica* (Liang et al., 2017). The cross-resistance spectrum between indoxacarb and metaflumizone is not clear: indoxacarb-selected *T. absoluta* strains exhibit only a limited Resistance Ratio (RR) increase for metaflumizone (Roditakis et al., 2017) whereas earlier studies of indoxacarb-resistant populations of *P. xylostella* indicate no cross-resistance to metaflumizone (Khakame et al., 2013). Conversely, a population of *Spodoptera exigua* with 942-fold resistance to metaflumizone exhibits only 16-fold resistance to indoxacarb (Su and Sun, 2014). On the other hand, selection of indoxacarb in the field confers cross-resistance to metaflumizone in at least one population of *P. xylostella* (Wang et al., 2016). There is evidence for synergistic effects of metabolic inhibitors on SCBI toxicity, implicating metabolic resistance mechanisms involving esterases or oxidases (Wang et al., 2016; Liang et al., 2017). However, synergists only partially reduced resistance against indoxacarb in *T. absoluta* (Roditakis et al., 2017) and their use suggested a limited role of detoxification in metaflumizone resistance in *Spodoptera exigua* (Su and Sun, 2014).

Resistance levels to both indoxacarb and metaflumizone are significantly correlated to the frequencies of two VGSC mutations, F1845Y and V1848I, identified in the domain IV S6 segment (Fig. 2), in two field populations of *P. xylostella* (Wang et al., 2016). The same mutations were identified in SCBI-resistant populations of *T. absoluta*, collected from tomato greenhouses from Italy and Greece (Roditakis et al., 2017). When F1845 and V1848 (*P. xylostella* numbering) mutations were tested using electrophysiology studies of heterologous expressed *B. germanica* VGSCs in *Xenopus* oocytes, it was found that F1845Y and

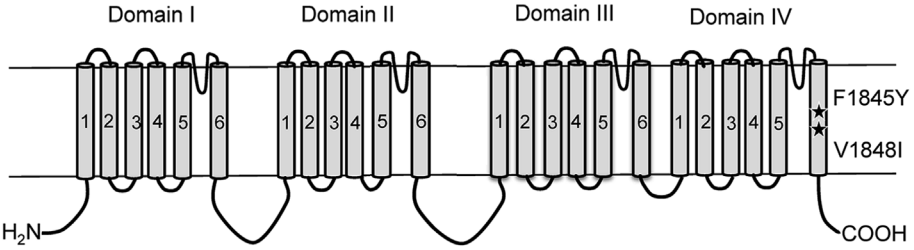

IVS6

PxNa$_v$	G	I	T	Y	L	L	S	Y	L	V	I	S	**F**	L	I	**V**	I	N	M	Y	I	A	V	I	L
TaNa$_v$	.	.	.	.	.	.	.	.	.	.	.	.	.	.	.	.	.	.	.	.	.	.	.	.	.
LepF1845Y	.	.	.	.	.	.	.	.	.	.	.	.	**Y**	.	.	.	.	.	.	.	.	.	.	.	.
LepV1848I	.	.	.	.	.	.	.	.	.	.	.	.	.	.	.	**I**	.	.	.	.	.	.	.	.	.
DmNa$_v$	.	.	.	**F**	.	.	.	.	.	.	.	.	.	.	.	.	.	.	.	.	.	.	.	.	.
DmF1845Y	.	.	.	**F**	.	.	.	.	.	.	.	.	**Y**	.	.	.	.	.	.	.	.	.	.	.	.
DmV1848I	.	.	.	**F**	.	.	.	.	.	.	.	.	.	.	.	**I**	.	.	.	.	.	.	.	.	.
AgNa$_v$	.	.	.	.	.	.	.	.	.	.	.	**A**	.	.	.	.	.	.	.	.	.	.	.	.	.
AmNa$_v$	.	.	**A**	.	.	.	.	.	.	.	.	.	.	.	.	.	.	.	.	.	.	.	.	.	.
TcNa$_v$	.	.	**A**	**F**	.	.	.	.	.	.	.	.	.	.	.	.	.	.	.	.	.	.	.	.	.
BgNa$_v$	.	.	**A**	**F**	.	.	.	.	.	.	.	.	.	.	.	.	.	.	.	.	.	.	.	.	.

Fig. 2. Positions of sodium channel mutations in the voltage-gated sodium channel (modified from Wang et al., 2016) and sequence alignment of the IVS6 segment. **A**: The sodium channel consists of four main domains (I–IV) and six transmembrane segments (S1−S6) within each domain. The two mutations in IVS6 related to sodium channel blocker insecticide resistance are shown. The amino acid positions are numbered based on a *Plutella xylostella* sequence (GenBank accession no. KM027335). **B**: Sequence alignment of the IVS6 segment of sodium channels from different insects. The mutation sites (F1845Y and V1848I) are shown in boxes. PxNa$_v$: *P. xylostella* (GenBank accession no. KM027335); TaNav: *Tuta absoluta* susceptible strain (Roditakis et al., 2017); LepF1845Y: Lepidopteran (*P. xylostella* and *T. absoluta*) sequence with mutation F1845Y); LepV1848I: Lepidopteran (*P. xylostella* and *T. absoluta* sequence with mutation V1848I); DmNa$_v$: *Drosophila melanogaster* (AAB59193.1); DmF1845Y: *D. melanogaster* sequence with mutation F1845Y; DmV1848I: *D. melanogaster* sequence with mutation V1848I. AgNa$_v$: *Anopheles gambiae* (CAM12801.1); AmNav: *Apis mellifera* (NP_001159377.1); TcNav: *Tribolium castaneum* (NP_001159380.1).BgNav: *Blattella germanica* (AAC47484.1).

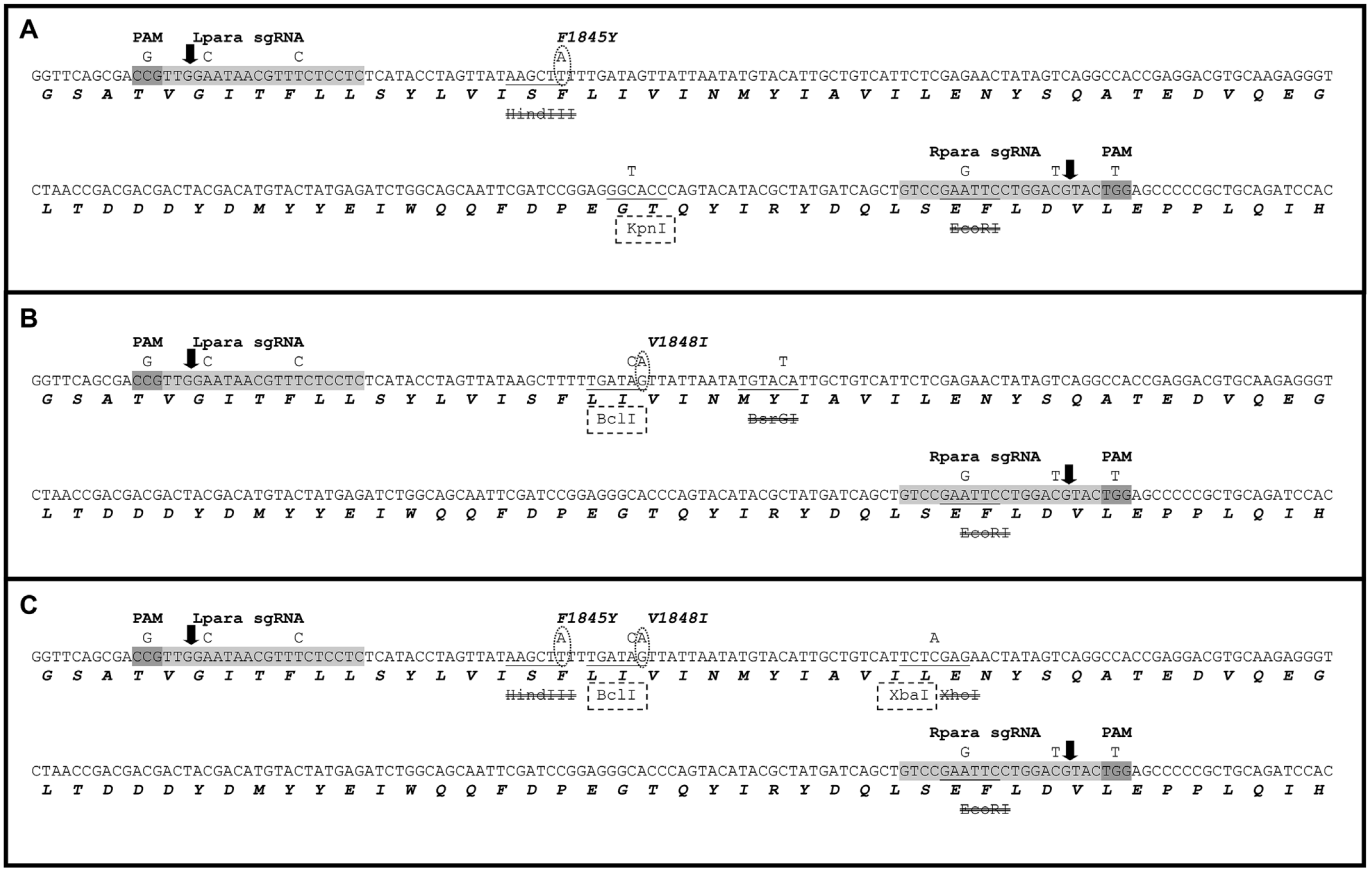

Fig. 3. CRISPR/Cas9 strategies for generation of genome modified flies bearing mutations F1845Y (A), V1848I (B), or both (C). Nucleotide and deduced amino acid sequence of a 258 bp fragment of *para* (corresponding to reverse complement of X: 16358465–16358722 at the BDGP6 genome assembly), flanking positions 1845 and 1848 (*P. xylostella* numbering) of the *Drosophila melanogaster* amino acid sequence. Light gray areas indicate the CRISPR/Cas9 targets selected (LPara sgRNA, Rpara sgRNA), while dark gray areas indicate the corresponding PAM (-*NGG*) triplets. Vertical arrows denote break points for CRISPR/Cas9-induced double stranded breaks. Ovals mark non-synonymous differences between target (wild-type) and donor (genome modified) sequences. Synonymous mutations incorporated for diagnostic purposes, as well as to avoid cleavage of the donor plasmid by the CRISPR/Cas9 machinery, are shown above the nucleotide sequence. Restriction sites abolished because of the genome modification are shown with double strikethrough letters and the corresponding sequence is underlined. Restriction sites introduced because of the genome modification are shown in dashed boxes and the corresponding sequence is also underlined.

V1848I (but not V1848A) reduced almost equally the inhibition of sodium current by indoxacarb, DCJW (an active metabolite of indoxacarb) and metaflumizone. This indicates that both these mutations might contribute to non-selective target-site resistance against both SCBIs. However, *in vivo* genetic functional validation of these mutations has not been documented so far.

In recent years, genome engineering through CRISPR/Cas9 technology has been employed in several insecticide resistance studies in model systems like *Drosophila* or in pest species where the technology has been established (reviewed in Perry and Batterham, 2018; Homem and Davies, 2018), providing useful information about the association of specific mutations with resistance against several insecticide classes, like spinosyns that target nicotinic acetylcholine receptor (Somers et al., 2015; Zimmer et al., 2016), etoxazole and benzoylureas targeting chitin synthase (Douris et al., 2016; Grigoraki et al., 2017) and diamides targeting ryanodine receptor (Douris et al., 2017; Zuo et al., 2017). In this study we have employed a CRISPR/Cas9 strategy in order to generate *Drosophila* strains bearing homozygous F1845Y or V1848I mutations in the *para* (voltage-gated sodium channel) gene, and performed toxicity bioassays on these strains in order to functionally validate resistance to SCBIs *in vivo*. We have also used molecular modeling studies to investigate SCBI interactions in the channel pore.

2. Materials and Methods

2.1. Chemicals

Chemical compounds used for contact bioassays were indoxacarb (Sigma-Aldrich, PubChem CID: 107,720) and metaflumizone (Sigma-Aldrich, PubChem CID: 11614934) (Fig. 1). The formulations used for feeding bioassays were Steward 30 WG (DuPont) for indoxacarb, and Alverde 24 SC (BASF) for metaflumizone.

2.2. Fly strains

The injections for genome modification of *Drosophila* were performed in preblastoderm embryos of the lab strain y1 M{nos-Cas9.P} ZH-2A w*, in which Cas9 is expressed under the control of *nanos* promoter (Port et al., 2014; further below referred as nos.Cas9, #54591 in Bloomington *Drosophila* stock center). Strain w + oc/FM7yBHw (kindly provided by Professor Christos Delidakis, IMBB and University of Crete) which contains the X chromosome balancer FM7c was used for genetic crosses and for keeping heterozygous mutants. The flies were kept at 25 °C temperature, at 60–70% humidity and 12:12 h photoperiod on a typical fly diet.

2.3. Amplification and sequencing of para target region

DNA from nos.Cas9 *Drosophila* adults was extracted with DNAzol (MRC) following the manufacturer instructions. Three sets of primers (Inv1F/R, Inv2F/R and Inv3F/R, Table S1) were designed based on the *para* gene sequence in order to amplify three overlapping fragments (Inv1-3) that add up to a 3134bp region encompassing genomic region X:16,466,144–16,463,017 of the *Drosophila* genome sequence (numbering according to BDGP6 genome assembly). The amplification reactions were performed using KapaTaq DNA Polymerase (Kapa Biosystems). The conditions were 95 °C for 2 min for initial denaturation followed by 30–35 cycles of denaturation at 95 °C for 30 s, annealing at 61°C-66 °C for 15 s, extension at 72 °C for 45–90 s and a final extension step for 2 min. The PCR products were purified with a PCR clean-up kit (Macherey-Nagel) according to manufacturer's instructions. Sequencing of the products was performed from both ends at StarSeq (Maintz, Germany).

2.4. Strategy for genome editing

An *ad hoc* CRISPR-Cas9 strategy was implemented in order to generate *Drosophila* strains bearing either one or both mutations (equivalent to F1845Y and V1848I found in *P. xylostella* and *T. absoluta*) in the *para* gene. We used the same CRISPR targets but different donor constructs for homologous-directed repair for the generation of each strain, containing either F1845Y or V1848I (or both, further below referred as FYVI). Based on the genomic sequence of *para* obtained for strain nos.Cas9, several CRISPR targets in the desired region were identified using the Optimal Target Finder online tool (Gratz et al., 2014, http://tools.flycrispr.molbio.wisc.edu/targetFinder). Two target sequences found upstream (Lpara) and downstream (Rpara) of the desired region in *para* gene were selected (Fig. 3) with no predicted off-target effects. In order to generate sgRNAs targeting those sequences, two different RNA expressing plasmids were generated based on the vector pU6-BbsI chiRNA (Gratz et al., 2013) following digestion with BbsI and ligation of two double stranded oligos, (dsLpara and dsRpara), which were generated by annealing single stranded oligos RparaF/RparaR and LparaF/LparaR (Table S1) respectively. Following ligation and transformation, single colonies for each construct were picked and checked for the correct insert by performing colony PCR using T7 universal primer and the reverse primer for each dsDNA. The sequence of each sgRNA expressing plasmid was verified by sequencing (Macrogen, Amsterdam).

Three different donor plasmids, paraF1845Y, paraV1848I and paraFYVI were synthesized *de novo* (Genscript) to facilitate Homologous Directed Repair for generation of strains F1845Y, V1848I and FYVI respectively (newly synthesized sequences were subcloned in pUC57 vector EcoRV site; relevant insert sequences for each donor plasmid are shown in Fig. S1). Each plasmid contained two ~1000 bp homology arms flanking the 228 bp target region between the two sgRNA targets Lpara and Rpara (Fig. 3). The target region was specifically designed in order to contain the desired mutations (F1845Y, V1848I or both in donor plasmids paraF1845Y, paraV1848I and paraFYVI respectively) along with certain additional synonymous mutations (see Fig. 3 for details) serving either as molecular markers (to facilitate molecular screening of CRISPR events), or to prevent unwanted CRISPR digestion of the donor itself.

2.5. Molecular screening and genetic crosses

Injection of nos.Cas9 pre-blastoderm embryos was performed at the IMBB/FORTH facility with injection mixes containing 75 ng/μl of each sgRNA expressing vector and 100 ng/μl of donor template. Hatched larvae were transferred into standard fly artificial diet and after 9–13 days G_0 surviving adults were collected and individually backcrossed with nos.Cas9 flies. In order to screen for CRISPR events, G_1 generation progeny from each cross were pooled into batches of ~30 and genomic DNA extraction was performed *en masse* in order to be screened with two different ways. Initially, 2 μg of genomic DNA were digested with HindIII (for F1845Y and FYVI crosses) or BsrGI (for V1848I); these enzymes cut only the wild type alleles but not potential mutant alleles in each DNA pool. Then, one strategy for screening consists of amplification with specific primers ParaSpecF/R (Table S1) that were designed taking into account the synonymous mutations introduced in the two sgRNA target sequences in all donor templates, in order to generate a diagnostic fragment of 250bp that is specific to genome modified alleles, but not wild-type ones. PCR was performed with Kapa Taq polymerase as previously described using ~60 ng of digested template DNA mix. An alternative strategy consists of PCR amplification with the "generic" primer pair ParaGenF/R (Table S1) which were designed in order to amplify a fragment of 752 bp that may be derived by either wild type (if still present, given the initial enzymatic cleavage of the template DNA mix) or genome modified alleles. Following PCR amplification, the product was digested with diagnostic enzymes introduced in the HDR donor sequence, namely KpnI for F1845Y (producing two diagnostic fragments of 536 bp and 217 bp), BclI for V1848I (producing two diagnostic fragments of 405 bp and 347 bp) and XbaI for FYVI (producing two fragments of 437 bp and 315 bp).

Crosses that proved positive for genome modified alleles were further explored in order to identify individual flies bearing mutant alleles and establish homozygous lines (see Fig. S2 for the whole crossing scheme). Individual G_1 flies from positive original G_0 crosses were backcrossed with nos.Cas9 and after generating G_2 progeny, they underwent molecular screening as previously described. Positive crosses now contain the mutant allele in 50% of the G_2 progeny. Individual female G_2 flies were then crossed with male flies carrying a balancer X chromosome (FM7c) with a characteristic phenotypic marker (*Bar*). After producing G_3 progeny, the female G_2 flies were again individually screened to identify positive crosses, and female G_3 flies potentially carrying the mutant allele opposite of an FM7c balancer were again back-crossed with male flies carrying FM7c balancer to produce G_4 progeny. One final round of molecular screening was performed to identify balanced lines containing the genome modified allele against FM7c, and G_5 adults were collected following phenotypic selection against the *Bar* marker and pooled in order to establish homozygous strains. DNA was extracted from several homozygous female and hemizygous male adults, amplified by using primers ParaGenF/R and the relevant amplification fragment was sequence verified (Macrogen, Amsterdam).

2.6. Toxicity bioassays

2.6.1. Contact bioassays

Insecticidal activity against adult flies was tested by residual contact application on nos.Cas9 flies. Test insecticides were dissolved in acetone and serial dilutions were prepared to make desired concentrations. A volume of 500 μl of each one was applied into glass scintillation vials. For each concentration there were 3 technical replicates. The vials were put on a roller for overlaying their entire surface for 30–40 min under a fume hood. Following the evaporation of acetone, 20 flies (10 males and 10 females, 1–3 day adults) were transferred into each vial. Individual vials were covered with a piece of cotton soaked into a solution of 5% sucrose. Vials were maintained at room temperature and flies were exposed for 24–96 h.

2.6.2. Feeding toxicity bioassays

For feeding bioassays, 2nd instar larvae were transferred in batches of 20 into fresh standard fly artificial food, supplemented with several concentrations of insecticide formulation solutions. Larval development, mortality, pupal eclosion, pupal size and adult survival were monitored and measured for 7–10 days. Each bioassay consisted of five to seven different concentrations, tested in triplicates. The control

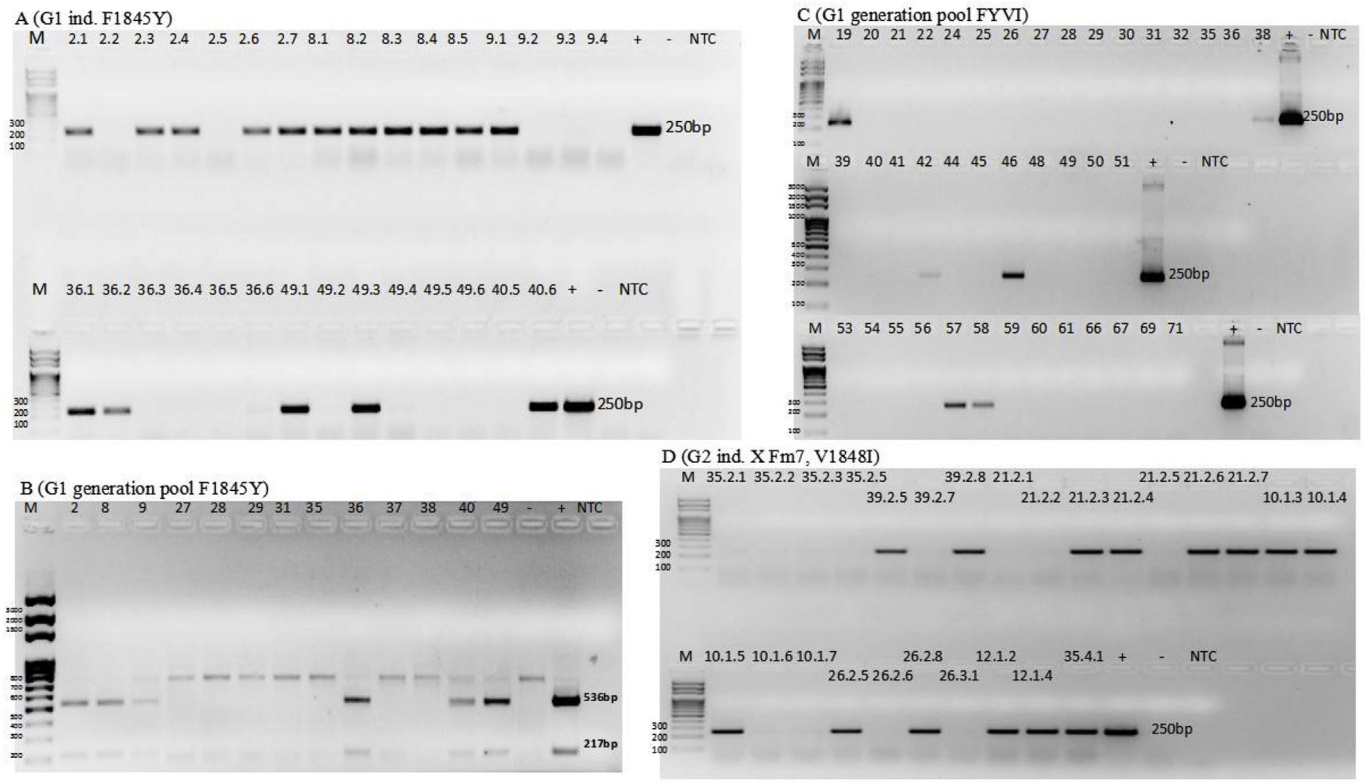

Fig. 4. Indicative diagnostic screening with specific primers yielding diagnostic PCR products in 2% agarose gel electrophoresis. M: molecular weight marker (100 bp ladder); +: positive control (PCR using as template the relevant donor plasmid for each mutation); -: negative control (PCR using as template DNA from non-injected nos.Cas9 flies; NTC: blank (no DNA template). (A) PCR screening yielding a 250 bp product of G_1 individuals backcrossed with nos.Cas9 originating from each original line (G_0) for the F1845Y mutation. (B) Diagnostic KpnI digestion of PCR product (752 bp) amplified with generic primers for massively screening G_1 progeny samples of injected G_0 flies yielding two diagnostic fragments of 536 bp and 217 bp. (C) PCR screening with specific primers (250 bp product) in pools of G_1 progeny of the original injected flies for the dual mutations FYVI. (D) PCR screening with specific primers (250 bp) of G_1 individuals for the mutation V1848I after cross with flies bearing balancer FM7c.

population (nos.Cas9) was tested along with the genome modified populations (F1845Y and V1848I); for each insecticide negative controls (no insecticide) were also included.

2.6.3. Statistical analyses

Concentration-response data of each bioassay setup were collected and analyzed with ProBit analysis using PoloPlus (LeOra Software, Berkeley, California) in order to calculate Lethal Concentrations of the 50% of the population subjected to the experiment (LC_{50} values), 95% fiducial limits (FL), linearity of the dose-mortality response, construction of mortality curves and statistical significance of the results.

2.7. Homology modeling and automated ligand docking

A homology model of the *Drosophila* para VGSC (UniProtKB accession P35500) was generated using the electric eel VGSC structure (PDB code 5XSY) as template. Sequences were aligned using ClustalW (Thompson et al., 1994) and are shown in Fig. S3. MODELLER (Eswar et al., 2007) was used to produce 50 initial homology models. The internal scoring function of MODELLER was used to select 10 models, which were visually inspected and submitted to the VADAR webserver (Willard et al., 2003) for assessment of stereochemical soundness in order to select the best model.

The 3-dimensional structure of metaflumizone was generated *ab initio* using MarvinSketch (version 5.9.1) of the ChemAxon suite (http://www.chemaxon.com). AutoDockTools (version 1.5.4) (Molecular Graphics Laboratory, Scripps Research Institute, La Jolla, CA, USA) was used to define rotatable bonds and merge non-polar hydrogens for metaflumizone. Automated ligand docking studies of metaflumizone with the *Drosophila para* model were performed using Auto-Dock Vina (version 1.1.2) (Trott and Olson, 2010) with a grid of 30 × 30 × 30 points (1 Å spacing) centered on the channel pore. F1845 and V1848 (*Plutella xylostella* numbering) side chains were allowed to flex during the docking run and subsequent docking predictions for metaflumizone were screened by selecting poses where the ligand was < 4.5 Å distance from these residues. Mutant channels with either the F1845Y or V1848I substitution were generated using Swiss-PdbViewer (Guex et al., 1999). Figures were produced using PyMOL (DeLano Scientific, San Carlos, CA, USA).

3. Results

3.1. Generation of Drosophila strains bearing mutations F1845Y and/or V1848I at the para gene

The mutations F1845Y and V1848I (*P. xylostella* numbering) in segment S6 of domain IV were introduced in *Drosophila* via a CRISPR/Cas9 coupled with Homologous Directed Repair (HDR) genome modification strategy. The *Drosophila para* VGSC sequence was aligned to the lepidopteran and other insect orthologs (Fig. 2B) and the target region identified. A genome modification strategy was designed in order to introduce the mutations under study (Fig. 3) and carried out as described in Materials and Methods (see 2.4 above).

Embryos of nos.Cas9 flies (expressing Cas9 under *nanos* promoter) were injected with three different plasmid mix combinations, each containing two sgRNA target plasmids (Lpara, Rpara) and one of the donor plasmids paraF1845Y, paraV1848I or paraFYVI (Fig. S1). For the F1845Y mutation, 55 adult flies derived from injected embryos (G_0)

were crossed with nos.Cas9 flies. Nine crosses were sterile, while the progeny of the remaining 46 (G_1) were screened with two different molecular screening approaches as described in 2.5. Six out of the 46 crosses were found to be positive for HDR. Regarding the V1848I mutation, 55 G_0 flies were crossed to nos.Cas9 and 21 of them were sterile. The remaining 34 crosses that provided G_1 progeny were screened and eight were positive for HDR. Finally, for FYVI (bearing both mutations), 71 crosses were set, 56 gave G_1 progeny and were screened, and six were found to be positive for HDR.

G_1 individuals originating from the original positive lines (G_0) were crossed, screened (Fig. 4) and then balanced in order to establish homozygous fly lines for each mutation (overall crossing scheme shown in Fig. S2). Following the final crosses in order to obtain homozygous modified flies, six lines homozygous for the F1845Y mutation and four lines homozygous for the V1848I mutation were established and sequence verified. However, for all five FYVI lines that were eventually generated bearing both mutations in the same allele, no homozygous females or hemizygous positive males were ever generated, and the FYVI allele had to be kept as heterozygote over balancer chromosome.

3.2. Validation of ability of F1845Y and V1848I mutations to confer resistance to SCBIs in Drosophila

In order to validate toxicity of SCBIs in *Drosophila*, contact bioassays were performed in 2–3 day old adult nos.Cas9 flies. No mortality was observed even after 96 h of continuous exposure to a concentration of 1000 μg/ml of either indoxacarb or metaflumizone.

Then, feeding toxicity bioassays were performed with 2nd instar larvae that were collected and transferred into fresh food containing several concentrations of each insecticide. *Drosophila* larvae were continuously in contact with the food supplemented with the insecticides. Toxicity effects such as cessation of feeding, larval paralysis, prolonged development and reduction of the size of pupae were observed. Since dead larvae cannot be readily visible inside the fly food, molting to pupae was considered a measurable proxy of eventual survival (most pupae eclose normally 7–10 days after the bioassay is initiated). Survival data underwent probit analysis and the corresponding LC_{50} values and resistance ratios versus the control (nos.Cas9) flies, along with 95% fiducial limits and associated statistics are shown in Table 1.

According to these findings, flies bearing the F1845Y mutation in homozygous (female)/hemizygous (male) state, exhibit 10.2-fold resistance to indoxacarb compared to nos.Cas9 wild type controls. On the other hand, the same flies exhibit much higher resistance to metaflumizone (RR: > 3400 with respect to nos.Cas9). Flies bearing the mutation V1848I, show similar moderate levels of resistance both to indoxacarb (RR: 6) and to metaflumizone (RR: 8.4) compared to wild-type (nos.Cas9) controls. These results were confirmed in several experiments using different fly lines bearing the mutations, with limited LC_{50} variation among different experiments, within the fiducial limits shown in Table 1.

3.3. Interactions of metaflumizone with wildtype and mutant para homology models

A homology model of the wild type *Drosophila* para VGSC was generated using the open-state electric eel VGSC structure (Yan et al., 2017). These channels share 57% sequence identity, as shown in the sequence alignment (Fig. S3) used for model generation. Docking predictions for metaflumizone in the open pore were generated and screened for interactions with the F1845 and V1848 residues. The top docking pose in terms of estimated binding energy (−10.6 kcal/mol estimated free energy of binding (ΔG_b)) is shown in Fig. 5.

Metaflumizone makes the majority of its binding contacts with residues on the DIV S6 helix, which include F1845, V1848, I1849 and Y1852 (*P. xylostella* numbering). These binding contacts are predominantly hydrophobic in nature, such as the interaction with the I1849 side chain that is orientated towards the DIII-DIV interface (Fig. 5C). One potential polar interaction is between the metaflumizone carbonyl group positioned near the side chain hydroxyl group of Y1852 (Fig. 5E), which raises the possibility of a hydrogen bond. The F1845 side chain and metaflumizone 4-cyanophenyl group are positioned to form an edge-to-face aromatic-aromatic interaction (Fig. 5C). Introducing the F1845Y substitution adds a hydroxyl group that extends the length of this side chain and consequently a steric clash was encountered with the docked ligand (Fig. 5D). The V1848 side chain interacts with the aromatic ring on the other end of metaflumizone molecule – the (trifluoromethoxy)phenyl group – and a steric clash was also found when V1848 was substituted with the larger V1848I side chain (Fig. 5E–F).

4. Discussion

Two mutations at the S6 segment of domain IV of VGSC (F1845Y and V1848I, *P. xylostella* numbering) have been reported in resistant populations of two pest species, *Plutella xylostella* (Wang et al., 2016) and *Tuta absoluta* (Roditakis et al., 2017) and have been implicated in SCBI resistance through *in vitro* studies where the relevant mutations are introduced in cockroach sodium channels expressed in *Xenopus* oocytes (Jiang et al., 2015). In the present study, we employed a reverse genetics approach to induce these mutations through CRISPR/Cas9 genome modification at the *para* gene of *Drosophila melanogaster* whose IVS6 sequence is very similar to the sequence of the two lepidopteran pests (Fig. 2B). We generated genome modified fly strains bearing each mutation and performed toxicity bioassays against two commercial SCBIs, indoxacarb and metaflumizone.

Our results (Table 1) provide direct *in vivo* confirmation that both F1845Y and V1848I have an effect on resistance against both commercial SCBIs. However, in contrast to previous *in vitro* characterization studies (Jiang et al., 2015), this effect is not uniform for each mutation/insecticide combination. Toxicity bioassays against different concentrations of indoxacarb indicate that both F1845Y and V1848I confer comparable, low to moderate ratios of resistance compared to wild-type controls (RR: 10.2 and 6 respectively). On the contrary, toxicity bioassays against metaflumizone indicate that although V1848I also confers resistance of similar scale (RR: 8.4), the F1845Y mutation has a much stronger impact by several orders of magnitude (RR: 3441.2), a result obtained in several independent experiments.

Although available *in vitro* evidence suggests that both mutations reduce the sensitivity of the cockroach channel to both insecticides (Jiang et al., 2015), the level of reduction is not substantially different

Table 1
Log-dose probit-mortality data for indoxacarb and metaflumizone against larvae of *Drosophila* genome modified strains F1845Y and V1848I versus nos.Cas9 control.

Compound	*Drosophila* strain	Slope ± SE	LC_{50} (95% CI) ug/ml	X^2 (df)	RR vs nos.Cas9
Indoxacarb	nos.Cas9	4.012 ± 0.360	2.756 (2.416–3.133)	17.406 (14)	1
	F1845Y	3.901 ± 0.370	28.202 (25.547–31.209)	14.782 (17)	10.2
	V1848I	4.270 ± 0.352	16.658 (15.124–18.434)	14.555 (22)	6
Metaflumizone	nos.Cas9	4.983 ± 0.598	0.525 (0.479–0.575)	9.375 (10)	1
	F1845Y	5.906 ± 0.798	1816.675 (1627.624–2017.529)	8.748 (16)	3441.2
	V1848I	2.964 ± 0.331	4.412 (3.763–5.131)	12.111 (13)	8.4

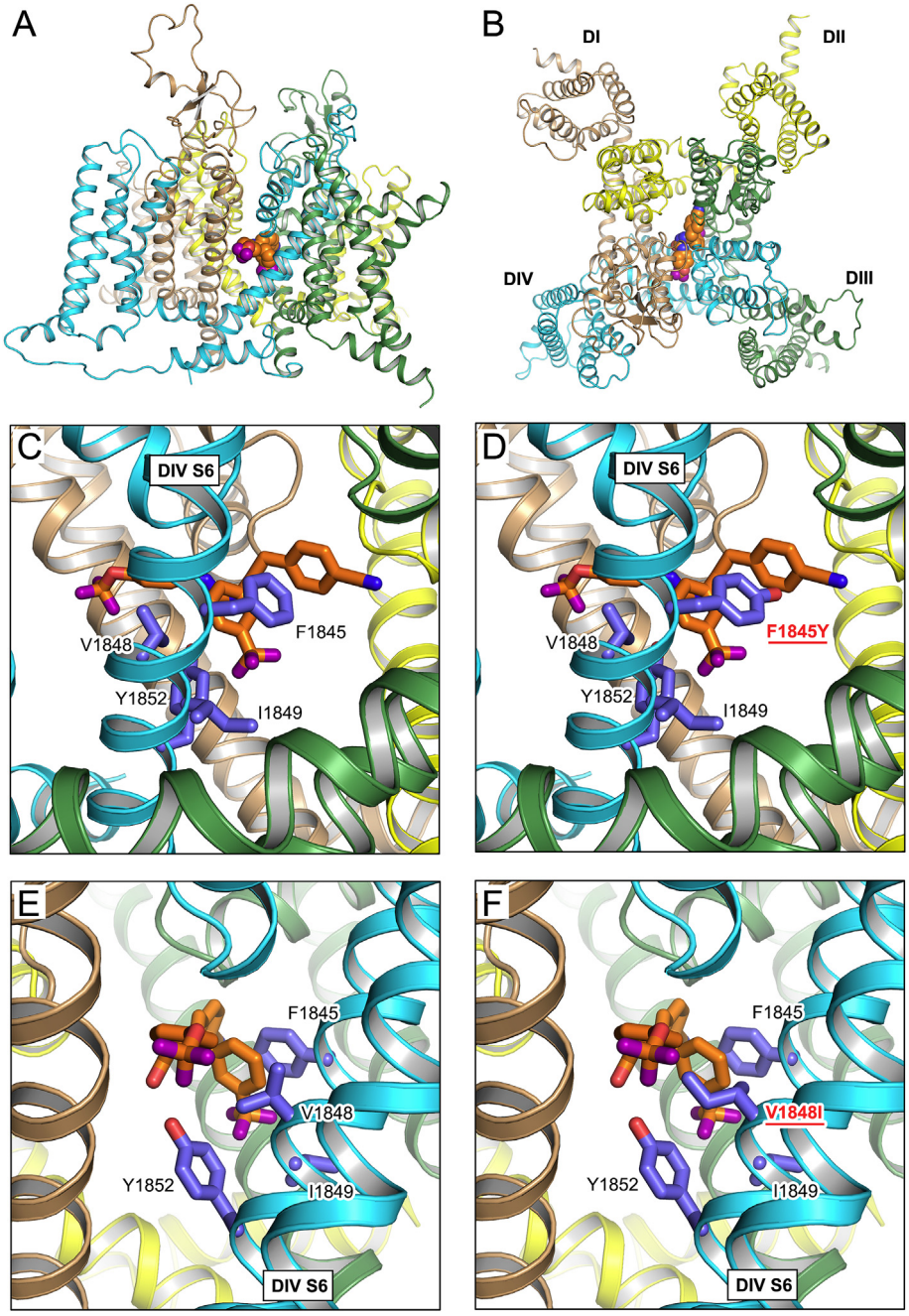

Fig. 5. Docking prediction of metaflumizone with *Drosophila para* VGSC homology models. (A–B) Transmembrane (A) and extracellular (B) view of the channel with each domain as differently colored ribbon and metaflumizone as orange spacefill. (C–D) Interaction of F1845 (C) and the substitution F1845Y (D) with metaflumizone. (E–F) Interaction of V1848 (E) and the substitution V1848I (F) with metaflumizone. Residues are numbered according to the *Plutella xylostella* channel. (For interpretation of the references to color in this figure legend, the reader is referred to the Web version of this article.)

among different mutation/insecticide combinations. Although the two approaches are not readily comparable, it is noteworthy that *in vitro* the percentage of inhibition by metaflumizone in F1845Y and V1848I mutant cockroach channels is virtually the same (Table 2 in Jiang et al., 2015), i.e. both mutations induce approximately the same reduction of sensitivity, in sharp contrast with the *in vivo Drosophila* bioassay results where F1845Y flies are > 400 times more resistant to metaflumizone compared to V1848I ones.

Given that the largest RR (> 3400) was found with metaflumizone and the F1845Y mutant, we employed molecular modeling studies to explore binding interactions of this ligand. Our docking pose for metaflumizone in the channel pore differs from that reported by Zhang et al. (2016), which used a homotetrameric bacterial VGSC structure as template for homology modeling, which was then opened *in silico* so that the pore adopted a conformation resembling that of the activated-state Kv1.2 channel. Our model is based on the open-state eukaryotic eel VGSC structure (Yan et al., 2017) that, in comparison with the Zhang model, has a narrower cytoplasmic entrance to the pore that metaflumizone is unlikely to fit through. Metaflumizone may still be able to access the pore through the large fenestration at the domain III-IV interface in our model, which was proposed by Zhang et al. (2016) as a possible ingress route given that metaflumizone can bind to resting sodium channels (von Stein et al., 2013). When docked in our model, metaflumizone did not make contact with a number of residues ($W^{1p52}A$, $V^{2i18}K$, $F^{3p44}A$, $T^{3i18}A$, $L^{4i8}A$; numbered according to Zhang et al. (2016)) that decrease the inhibition effect of metaflumizone when

mutated (von Stein and Soderlund, 2012; Zhang et al., 2016). This identifies a potential limitation of our model, which is that binding contacts present in the more widely-opened pore described by Zhang et al. (2016) may not be positioned to interact with metaflumizone in our model. Conversely, in our different conformation of the open pore, we identified potential new interactions between DIV S6 residues and metaflumizone, including a possible hydrogen bond with Y1852 and also an interaction with I1849, which was previously identified as a possible determinant of SCBI species-selectivity as it is not conserved as isoleucine in mammals (Zhang et al., 2016). As previously suggested by Zhang et al. (2016), the resistance associated with the V1848I mutation may be due to a steric hindrance mechanism that inhibits metaflumizone binding; a steric clash with the ligand was found when this mutation was introduced into our model. A steric clash was also found with the F1845Y mutation and the introduction of the hydrophilic hydroxyl group on this side chain raises the possibility that hydrophobic repulsion with metaflumizone may also impede ligand binding. The F1845Y clash is with the 4-cyanophenyl moiety of metaflumizone that is absent from indoxacarb/DCJW (Fig. 1), which may explain the difference between the RR > 3400 of metaflumizone versus RR 10.6 for indoxacarb in flies with F1845Y. As mentioned, a major difference between the inhibitory effect of SCBIs on the equivalent F1845Y mutant of the cockroach VGSC was not found by Jiang et al. (2015). Future electrophysiology studies may determine if there is some inherent difference in the pharmacology of BgNav1-1 vs *para* VGSCs towards SCBIs, despite the sequences of their DIV S6 segments being essentially identical.

Our effort to generate a homozygous fly strain carrying both mutations at the same allele (in *cis*) was not successful; although such a "dual" allele has been generated by CRISPR/Cas9 coupled with homologous recombination, it was always found in heterozygotes and no homozygous flies bearing both mutations in *cis* could be generated. Interestingly, heterozygotes from resistant populations of *P. xylostella* have also been found to always have the two mutations in *trans* (single) and never in *cis* ("dual" allele; Wang et al., 2016), and similarly in resistant *T. absoluta* (data not shown; samples from Roditakis et al., 2017) This is a strong indication that the two mutations are mutually exclusive, i.e. that the "dual" allele bearing both mutations is not viable, leading to a non-functional VGSC.

Drosophila is versatile system that enables multiple questions to be addressed in a common genetic framework, providing the sophisticated toolkit required for such an operation. The establishment of genome modification technology in insecticide resistance studies in combination with standard genetic engineering may facilitate validation of target-site resistance to SCBIs (as in this study) as well as co-existing synergistic mechanisms of metabolic resistance as soon as candidate genes for these become available for investigation.

Conflicts of interest

The authors declare no conflict of interest.

Acknowledgments

The authors wish to thank Ioannis Livadaras (IMBB/FORTH) for the injections performed in *Drosophila* embryos and Professor Christos Delidakis (IMBB/FORTH, University of Crete) for providing us with balancer fly stocks and useful tips. Part of this work was financially supported by the Stavros Niarchos Foundation within the framework of the project ARCHERS ("Advancing Young Researchers' Human Capital in Cutting Edge Technologies in the Preservation of Cultural Heritage and the Tackling of Societal Challenges") as a PhD fellowship to GRS, as well as by a GSRT (General Secretariat for Research and Technology, Greece) "Kripis" research program for the development of research institutes (to IMBB-FORTH).

Appendix A. Supplementary data

Supplementary data to this article can be found online at https://doi.org/10.1016/j.ibmb.2018.12.008.

References

Ahmad, M., Hollingworth, R.M., Wise, J.C., 2002. Broad-spectrum insecticide resistance in obliquebanded leafroller *Choristoneura rosaceana* (Lepidoptera: Tortricidae) from Michigan. Pest Manag. Sci. 58, 834–838. https://doi.org/10.1002/ps.531.

Bird, L.J., Drynan, L.J., Walker, P.W., 2017. The Use of F_2 Screening for Detection of Resistance to Emamectin Benzoate, Chlorantraniliprole, and Indoxacarb in Australian Populations of *Helicoverpa armigera* (Lepidoptera: Noctuidae). J. Econ. Entomol. 110, 651–659. https://doi.org/10.1093/jee/tox037.

Carnevale, V., Klein, M.L., 2017. Small molecule modulation of voltage gated sodium channels. Curr. Opin. Struct. Biol. 43, 156–162. https://doi.org/10.1016/j.sbi.2017.02.002.

Catterall, W.A., 2017. Forty Years of Sodium Channels: Structure, Function, Pharmacology, and Epilepsy. Neurochem. Res. 42, 2495–2504. https://doi.org/10.1007/s11064-017-2314-9.

Douris, V., Steinbach, D., Panteleri, R., Livadaras, I., Pickett, J.A., Van Leeuwen, T., Nauen, R., Vontas, J., 2016. Resistance mutation conserved between insects and mites unravels the benzoylurea insecticide mode of action on chitin biosynthesis. Proc. Natl. Acad. Sci. U.S.A. 113, 14692–14697. https://doi.org/10.1073/pnas.1618258113.

Douris, V., Papapostolou, K.M., Ilias, A., Roditakis, E., Kounadi, S., Riga, M., Nauen, R., Vontas, J., 2017. Investigation of the contribution of RyR target-site mutations in diamide resistance by CRISPR/Cas9 genome modification in *Drosophila*. Insect Biochem. Mol. Biol. 87, 127–135. https://doi.org/10.1016/j.ibmb.2017.06.013.

Eswar, N., Webb, B., Marti-Renom, M.A., Madhusudhan, M.S., Eramian, D., Shen, M.-Y., Pieper, U., Sali, A., 2007. Comparative protein structure modeling using MODELLER. Curr Protoc Protein Sci Chapter 2 Unit 2.9. https://doi.org/10.1002/0471140864.ps0209s50.

Gawali, V.S., Lukacs, P., Cervenka, R., Koenig, X., Rubi, L., Hilber, K., Sandtner, W., Todt, H., 2015. Mechanism of modification, by lidocaine, of fast and slow recovery from inactivation of Voltage-Gated Na+ Channels. Mol. Pharmacol. 88, 866–879. https://doi.org/10.1124/mol.115.099580.

Gratz, S.J., Cummings, A.M., Nguyen, J.N., Hamm, D.C., Donohue, L.K., Harrison, M.M., Wildonger, J., O'Connor-Giles, K.M., 2013. Genome engineering of *Drosophila* with the CRISPR RNA-guided Cas9 nuclease. Genetics 194, 1029–1035. https://doi.org/10.1534/genetics.113.152710.

Gratz, S.J., Ukken, F.P., Rubinstein, C.D., Thiede, G., Donohue, L.K., Cummings, A.M., O'Connor-Giles, K.M., 2014. Highly specific and efficient CRISPR/Cas9-catalyzed homology-directed repair in *Drosophila*. Genetics 196, 961–971. https://doi.org/10.1534/genetics.113.160713.

Grigoraki, L., Puggioli, A., Mavridis, K., Douris, V., Montanari, M., Bellini, R., Vontas, J., 2017. Striking diflubenzuron resistance in *Culex pipiens*, the prime vector of West Nile Virus. Sci. Rep. 7, 11699. https://doi.org/10.1038/s41598-017-12103-1.

Guex, N., Diemand, A., Peitsch, M.C., 1999. Protein modelling for all. Trends Biochem. Sci. 24, 364–367. https://doi.org/10.1016/S0968-0004(99)01427-9.

Hempel, K., Hess, F.G., Bögi, C., Fabian, E., Hellwig, J., Fegert, I., 2007. Toxicological properties of metaflumizone. Vet. Parasitol. 150, 190–195. https://doi.org/10.1016/j.vetpar.2007.08.033.

Homem, R.A., Davies, T.G.E., 2018. An overview of functional genomic tools in deciphering insect resistance. Curr. Opin. Insect Sci. 27, 103–110. https://doi.org/10.1016/j.cois.2018.04.004.

Jiang, D., Du, Y., Nomura, Y., Wang, X., Wu, Y., Zhorov, B.S., Dong, K., 2015. Mutations in the transmembrane helix S6 of domain IV confer cockroach sodium channel resistance to sodium channel blocker insecticides and local anesthetics. Insect Biochem. Mol. Biol. 66, 88–95. https://doi.org/10.1016/j.ibmb.2015.09.011.

Khakame, S.K., Wang, X., Wu, Y., 2013. Baseline toxicity of metaflumizone and lack of cross resistance between indoxacarb and metaflumizone in diamondback moth (Lepidoptera: Plutellidae). J. Econ. Entomol. 106, 1423–1429. http://doi.org/10.1603/EC12494.

Liang, D., McGill, J., Pietri, J.E., 2017. Unidirectional cross-resistance in german cockroach (Blattodea: Blattellidae) populations under exposure to insecticidal baits. J. Econ. Entomol. 110, 1713–1718. https://doi.org/10.1093/jee/tox144.

Perry, T., Batterham, P., 2018. Harnessing model organisms to study insecticide resistance. Curr. Opin. Insect Sci. 27, 61–67. https://doi.org/10.1016/j.cois.2018.03.005.

Port, F., Chen, H.M., Lee, T., Bullock, S.L., 2014. Optimized CRISPR/Cas tools for efficient germline and somatic genome engineering in *Drosophila*. Proc. Natl. Acad. Sci. U. S. A 111, E2967–E2976. https://doi.org/10.1073/pnas.1405500111.

Roditakis, E., Mavridis, K., Riga, M., Vasakis, E., Morou, E., Rison, J.L., Vontas, J., 2017. Identification and detection of indoxacarb resistance mutations in the *para* sodium channel of the tomato leafminer. *Tuta absoluta*: Pest Manag. Sci. 73, 1679–1688. https://doi.org/10.1002/ps.4513.

Shen, H., Zhou, Q., Pan, X., Li, Z., Wu, J., Yan, N., 2017. Structure of a eukaryotic voltage-gated sodium channel at near-atomic resolution. Science 355 eaal4326. https://doi.org/10.1126/science.aal4326.

Shen, H., Li, Z., Jiang, Y., Pan, X., Wu, J., Cristofori-Armstrong, B., Smith, J.J., Chin, Y.K.Y., Lei, J., Zhou, Q., King, G.F., Yan, N., 2018. Structural basis for the modulation of voltage-gated sodium channels by animal toxins. Science eaau2596. July 26, 2018. https://doi.org/10.1126/science.aau2596.

Shono, T., Zhang, L., Scott, J.G., 2004. Indoxacarb resistance in the house fly, *Musca domestica*. Pestic. Biochem. Physiol. 80, 106–112. https://doi.org/10.1016/j.pestbp.2004.06.004.

Silver, K.S., Soderlund, D.M., 2007. Point mutations at the local anesthetic receptor site modulate the state-dependent block of rat Nav1.4 sodium channels by pyrazoline-type insecticides. Neurotoxicology 28, 655–663. https://doi.org/10.1016/j.neuro.2007.02.001.

Silver, K.S., Song, W., Nomura, Y., Salgado, V.L., Dong, K., 2010. Mechanism of action of sodium channel blocker insecticides (SCBIs) on insect sodium channels. Pestic. Biochem. Physiol. 97, 87–92. https://doi.org/10.1016/j.pestbp.2009.09.001.

Silver, K., Dong, K., Zhorov, B.S., 2017. Molecular mechanism of action and selectivity of Sodium Channel Blocker Insecticides. Curr. Med. Chem. 24, 2912–2924. https://doi.org/10.2174/0929867323666161216143844.

Somers, J., Nguyen, J., Lumb, C., Batterham, P., Perry, T., 2015. *In vivo* functional analysis of the *Drosophila melanogaster* nicotinic acetylcholine receptor Dα6 using the insecticide spinosad. Insect Biochem. Mol. Biol. 64, 116–127. https://doi.org/10.1016/j.ibmb.2015.01.018.

Su, J.Y., Sun, X.X., 2014. High level of metaflumizone resistance and multiple insecticide resistance in field populations of *Spodoptera exigua* (Lepidoptera: Noctuidae) in Guangdong Province, China. Crop Protect. 61, 58–63. https://doi.org/10.1016/j.cropro.2014.03.013.

Thompson, J.D., Higgins, D.G., Gibson, T.J., 1994. CLUSTAL W: improving the sensitivity of progressive multiple sequence alignment through sequence weighting, position-specific gap penalties and weight matrix choice. Nucleic Acids Res. 22, 4673–4680. https://doi.org/10.1093/nar/22.22.4673.

Tian, X., Sun, X., Su, J., 2014. Biochemical mechanisms for metaflumizone resistance in beet armyworm, *Spodoptera exigua*. Pestic. Biochem. Physiol. 113, 8–14. https://doi.org/10.1016/j.pestbp.2014.06.010.

Trott, O., Olson, A.J., 2010. AutoDock Vina: improving the speed and accuracy of docking with a new scoring function, efficient optimization, and multithreading. J. Comput. Chem. 31, 455–461. https://doi.org/10.1002/jcc.21334.

von Stein, R.T., Soderlund, D.M., 2012. Compound-specific effects of mutations at Val787 in DII-S6 of Nav 1.4 sodium channels on the action of sodium channel inhibitor insecticides. Neurotoxicology 33, 1381–1389. https://doi.org/10.1016/j.neuro.2012.09.003.

von Stein, R.T., Silver, K.S., Soderlund, D.M., 2013. Indoxacarb, metaflumizone, and other sodium channel inhibitor insecticides: Mechanism and site of action on mammalian voltage-gated sodium channels. Pestic. Biochem. Physiol. 106, 101–112. https://doi.org/10.1016/j.pestbp.2013.03.004.

Wang, X.-L., Su, W., Zhang, J.-H., Yang, Y.-H., Dong, K., Wu, Y.-D., 2016. Two novel sodium channel mutations associated with resistance to indoxacarb and metaflumizone in the diamondback moth, *Plutella xylostella*. Insect Sci. 23, 50–58. https://doi.org/10.1111/1744-7917.12226.

Willard, L., Ranjan, A., Zhang, H., Monzavi, H., Boyko, R.F., Sykes, B.D., Wishart, D.S., 2003. VADAR: a web server for quantitative evaluation of protein structure quality. Nucleic Acids Res. 31, 3316–3319. https://doi.org/10.1093/nar/gkg565.

Yan, Z., Zhou, Q., Wang, L., Wu, J., Zhao, Y., Huang, G., Peng, W., Shen, H., Lei, J., Yan, N., 2017. Structure of the Nav1.4-β1 complex from electric eel. Cell 170, 470–482. e11. https://doi.org/10.1016/j.cell.2017.06.039.

Zhang, T., Wang, Z., Wang, L., Luo, N., Jiang, L., Liu, Z., Wu, C.-F., Dong, K., 2013. Role of the DSC1 channel in regulating neuronal excitability in *Drosophila melanogaster*: Extending nervous system stability under stress. PLoS Genet. 9, e1003327. https://doi.org/10.1371/journal.pgen.1003327.

Zhang, Y., Du, Y., Jiang, D., Behnke, C., Nomura, Y., Zhorov, B.S., Dong, K., 2016. The receptor site and mechanism of action of sodium channel blocker insecticides. J. Biol. Chem. 291, 20113–20124. https://doi.org/10.1074/jbc.M116.742056.

Zhang, S., Zhang, X., Shen, J., Li, D., Wan, H., You, H., Li, J., 2017. Cross-resistance and biochemical mechanisms of resistance to indoxacarb in the diamondback moth. *Plutella xylostella*. Pestic. Biochem. Physiol. 140, 85–89. https://doi.org/10.1016/j.pestbp.2017.06.011.

Zimmer, C.T., Garrood, W.T., Puinean, A.M., Eckel-Zimmer, M., Williamson, M.S., Davies, T.G.E., Bass, C., 2016. A CRISPR/Cas9 mediated point mutation in the alpha 6 subunit of the nicotinic acetylcholine receptor confers resistance to spinosad in *Drosophila melanogaster*. Insect Biochem. Mol. Biol. 73, 62–69. https://doi.org/10.1016/j.ibmb.2016.04.007.

Zuo, Y., Wang, H., Xu, Y., Huang, J., Wu, S., Wu, Y., Yang, Y., 2017. CRISPR/Cas9 mediated G4946E substitution in the ryanodine receptor of *Spodoptera exigua* confers high levels of resistance to diamide insecticides. Insect Biochem. Mol. Biol. 89, 79–85. https://doi.org/10.1016/j.ibmb.2017.09.005.